# Ambient noise tomography from the first two years of the USArray Transportable Array: Group speeds in the western US

M.P. Moschetti[1†], M.H. Ritzwoller[1], and N.M. Shapiro[2]

1 - Center for Imaging the Earth's Interior, Department of Physics, University of Colorado at Boulder, Campus Box 390, Boulder, CO 80309, USA

2 - Laboratoire de Sismologie, CNRS, IPGP, 4 place Jussieu, 75005 Paris, France.

† To whom correspondence should be directed: morganm@ciei.colorado.edu, 303-735-3048

Submitted to *Geophysical Research Letters*: September 27, 2006.

## Abstract

We have applied ambient noise surface wave tomography to data that have emerged continuously from the EarthScope USArray Transportable Array (TA) over the past two years. Using continuous seismic records from TA stations in the western United States between October 2004 and July 2006, we assess the effect on estimated group speed maps of the expansion of the TA. Estimated Green's functions are calculated by cross-correlationing noise records between every station pair. Within the 5 to 50 second period band, we measure the dispersion characteristics of Rayleigh waves using a frequency-time analysis method. We present the group velocity maps at periods of 8-, 16-, and 24-second. We demonstrate that the foot-print of the TA encloses a region with resolution at about the average inter-station spacing ($\sim$ 75 km). This region of high resolution has increased during the operation of the TA by a factor of between 5 and 7 and is continuing to grow as the TA moves eastward across the US. Geological features correlate strongly with velocity anomalies in the group speed maps.

## Introduction

Ambient noise surface wave tomography is an effective technique to estimate surface wave dispersion maps at multiple spatial scales over a broad period band (e.g., Sabra et al., 2005; Shapiro et al., 2005; Cho et al., 2006; Lin et al., 2006; Yang et al., 2006; Yao et al., 2006). The technique provides a means to make observations of short period surface waves along inter-station paths, which are inaccessible by earthquake tomography. Because earthquakes are primarily limited to plate margins and tectonically-active regions, the tomography of tectonically-quiescent regions requires the observation of teleseisms or the use of active sources. Shorter period surface waves, which are most sensitive to the crust, are preferentially attenuated and scattered, often leading to poor constraints on the crust from teleseismic earthquake observations. In addition, the distribution of azimuths from earthquakes is restricted by the timing and location of natural events. In contrast with traditional earthquake surface wave tomography, ambient noise tomography is limited by the number and path density of inter-station paths. For the technique to provide high resolution results across large areas requires both dense instrumentation and widely-distributed stations.

Most ambient noise studies have made use of data from well-established regional and national networks, which are limited by station spacing and distribution. A small number of highly-instrumented regions, such as southern California, exist and provide dense station coverage on a local to regional scale, but do not provide sufficient coverage to produce images of larger regions, such as the western United States. In fact, large regions of the United States are poorly instrumented, making short-period ambient noise measurements for high resolution tomography impossible.

The emerging EarthScope USArray Transportable Array (TA) provides a nearly ideal network for the application of ambient noise surface wave tomography to provide new information about the crust and uppermost mantle. The station coverage provided by the TA and other networks for this study is shown in Figure 1. Station density

is approximately uniform across the network, and excellent spatial and azimuthal coverage emerges from inter-station paths. Average station spacing is approximately 70 kilometers, and once built-out, 400 stations will be deployed simultaneously. Installation of the first TA stations occurred in 2004, and the network has been expanding across the western United States ever since. TA instruments now cover California and much of Oregon, Washington, and Nevada, and the network continues to grow at an average rate of about two stations each week.

We investigate here the applications and limitations of ambient noise measurements to a dense, expanding network, and examine changes to the resolution and group velocity maps as the network has grown. The study utilizes stations from the TA and several regional networks to generate estimated Green's functions from data sets for October 2004 and a cumulative stack of up to twenty-two months of data from October 2004 through July 2006. Group speed dispersion curves are measured in the 5- to 50-second period band. We present here the resolution and group velocity maps at 8-, 16-, and 24-second periods.

## Methods and Data Processing

The ambient noise data processing that precedes surface wave tomography is based on the cross-correlation of observations of long time-sequences of ambient noise to extract estimated Green's functions. The dispersion characteristics of the estimated Green's functions provide information about the wave propagation between the stations and, hence, about seismic velocities in the crust and uppermost mantle. We process day-length seismic records from the TA and several regional networks from the western US region as continuous, vertical-component waveforms. For the purpose of this paper, we define the western US by the coordinate boundaries: 30 to 100 degrees latitude, and -126 to -110 degrees longitude. By restricting data processing to vertical-component waveforms within the 5- to 50-second period band, we recover only Rayleigh wave

arrivals.

Data processing closely follows the methodology described by Bensen et al. (2006). Temporal normalization to remove the effects of earthquakes and instrumental irregularities is carried out by the running-absolute-mean normalization method (Bensen et al., 2006) on instrument response-corrected records. We pre-whiten the amplitude spectra to broaden the period range for dispersion measurements. Cross-correlations are carried out in the 5- to 100-second period band for every station pair. Day-long cross-correlations are stacked to produce cumulative time-series containing up to twenty-two months of waveform data. Station downtime and growing station coverage result in significant variation in the time-series lengths for different station-pairs. Cross-correlation waveforms present signal on both positive and negative lags, i.e., the causal and acausal signals, respectively, corresponding to waves propagating in opposite directions between the stations. Example cross-correlograms are shown in Figure 2. Because of the seasonal variation in the amplitude and spectral content of these signals, we average the causal and acausal signals to yield the symmetric-component, which is used for all subsequent processing.

Group velocity dispersion measurements are obtained using an automated frequency-time analysis (FTAN) method (e.g., Ritzwoller and Levshin, 1998) based on earthquake dispersion measurement (Bensen et al, 2006). The automated FTAN method is performed in two stages. The first measurement is made on the raw, symmetric-component signal, and the measured dispersion curve is used to construct a phase-matched filter. The second measurement is made on the phase-matched filtered signal to yield the final group velocity dispersion curve.

Selection of dispersion curves for the estimation of group speed maps differs slightly from that of Bensen et al. (2006) because the TA data set changes with time. Bensen et al. (2006) promote a selection criterion based on formal uncertainties defined from the variation in the seasonally-averaged dispersion curves. This method requires

at least one-year record segments. Because long record segments are not available for the newly-installed stations of the TA, we use signal-to-noise ratios as a proxy for uncertainties. We select group velocity measurements based on two criteria. (1) The inter-station spacings determine the maximum period accepted from individual dispersion curves. Three wavelengths is the minimum acceptable inter-station spacing. (2) Each group velocity measurement must derive from a cross-correlogram that exceeds a spectral signal-to-noise ratio threshold. The threshold for the October 2004 data set is 12, and the threshold for the data set from October 2004 through July 2006 is 20.

Once the dispersion curves are selected, tomography is carried out on a half-degree-by-half-degree grid to generate group speed maps. Tomography proceeds in two steps. The first step of tomography generates overly-smoothed maps which are then used to identify and reject group velocity measurements for which the travel time residuals are more than 15 seconds. The standard deviation for time residuals in four distance bins are then computed, and we reject those measurements for which the time residual is greater than three standard deviations from the mean. The remaining measurements are used for the second step of tomography, which yields the final group velocity maps based on the tomographic method of Barmin et al. (2001).

## Results and Discussion

The collection of ambient noise records began in October 2004 and continued through July 2006. During the study period, the number of stations included in the data stacks increased from 90 to 252. The stations contributing records to the inversions are plotted in Figure 1. The duration that noise records are available from each station is represented by the station symbol color. The evolution of the TA during the study period is reflected by the time that records are available; most southern and central California stations were installed prior to October 2004, and the network expanded to the north and east during the study period.

Cross-correlations of daily records are carried out between all stations and are stacked to generate the study data sets. The October 2004 data set comprises a month stack of data records, and the October 2004 to July 2006 data set comprises stacks of up to twenty-two months in length – although the vast majority of stacks are much shorter. There is considerable variability in time-series length in the latter data set. Daily records for which at least 90% of the data is not available are excluded from the stack. The number of inter-station cross-correlations increased from 4068 to 30261 during the study period.

Examples of the full cross-correlation waveforms are provided in Figure 2a. The four waveforms presented are selected from four geological terranes (the Cascades, the Basin and Range, the Central Valley, and the Sierras). The waveforms presented result from time stacks of 3.4, 2.1, 17.5, and 13.6 months of data, respectively, because of the expansion of the TA. The asymmetric nature of the cross-correlations results from differences in the ambient noise sources in the two opposing directions along the inter-station axis. Using the Cascades waveform in Figure 2a as an example (C05A is the northern station), the positive lag represents the wave propagation from C05A to G05A, and the negative lag represents the reverse propagation. The larger amplitude of the negative lag suggests that the dominant noise source originates from the south during the 3.4 months of joint operation of these two stations. Aspects of ambient noise sources derived from long range correlation properties have been characterized by several investigators (e.g., Shapiro et al., 2006; Stehly et al, 2006; Yang and Ritzwoller, 2006).

Group velocity dispersion measurements are made on the phase-matched filtered cross-correlograms between 5- and 50-second periods. Not all cross-correlation waveforms produce dispersion measurements; group velocity measurements fail due to low signal levels and contamination by coherent, off-axis noise sources. Four example dispersion measurements are presented in Figure 2b. Only measurements in which a minimum

of three wavelengths separate stations are accepted. The different period bands of the dispersion curves in Figure 2b reflect this distance criterion.

Although qualitative interpretation of dispersion curves in terms of Earth structure is difficult, some insight into local crustal structure may be gained from the curves in Figure 2b. Primarily, one looks at the short periods, and the slope near 25 seconds, which are sensitive to surface sedimentary deposits (or lack thereof) and crustal thickness, respectively. The curves from the Cascades and the Sierras show high short period group speeds, suggesting an absence of, or thin, sedimentary deposits. The shallow slope of the Sierran dispersion curve suggests a thick crust along the propagation path. The very slow short period group speeds from the Central Valley suggest thick, sedimentary deposits; the large slope of the curve results from the increasing sensitivity of the surface waves to basement material with increasing wave period. The surface deposits in the Basin and Range appear to be intermediate in group velocity to the crystalline rocks of the Sierras and Cascades and the sediments of the Central Valley.

For a dispersion measurement to be used in the tomographic inversion, the spectral signal-to-noise ratio (SNR) at the period must exceed the threshold value or the measurement is rejected. Examples of SNRs for each of the cross correlations at 16 seconds period are listed in Figure 2a. The continuous addition of new stations to the TA makes the uncertainty-based rejection procedure of Bensen et al (2006) inappropriate for this work. In the absence of meaningful uncertainty estimates, we use a higher signal-to-noise threshold than advocated by Bensen et al. (2006) in order to be more conservative in the initial selection of waveforms.

This process resulted in the selection of between 45% and 55% of the original cross-correlograms for further data processing. Additional data selection is based on the time residuals derived from an over-smoothed tomography map. At 8-second period, the number of paths used for the inversion increased from 1952, using data from October 2004, to 13356, using data from October 2004 to July 2006. The number of paths at 16-

and 24-second periods increased from 1815 to 16442, and 1035 to 13590, respectively. These numbers represent paths which exceed the distance and signal-to-noise criteria and whose computed time residuals are within three standard deviations of the average for their distance bin. The majority of rejected measurements result from poor signal quality and insufficient station spacing. Table 1 summarizes the number of paths rejected at each of the four steps in data processing.

Resolution maps are constructed using the resulting data set at periods of 8-, 16-, and 24-sec, using the method of Barmin et al. (2001) and modified by Levshin et al. (2005). Each row of the resolution matrix is taken as a resolution kernel for one node in the inversion. We fit a 2-D symmetric Gaussian function to the resolution surface at each node and report the resolution as twice the standard deviation. A comparison between the 8-second period resolution map from October 2004 with that from the October 2004 to July 2006 data set is presented in Figure 3. The contour line designates a resolution of 75 km and encloses the region of high resolution. The high resolution areas increase by factors of 5.75 (8-sec), 5.35 (16-sec), and 6.98 (24-sec), comparing the maps from October 2004 to the maps using data from October 2004 to July 2006.

The group velocity maps for the 8-second period and the 16- and 24-second periods are presented in Figures 4 and 5. Maps at all periods and time intervals are damped similarly. The travel time misfits for the group velocity maps presented here are 4.6, 2.7, and 3.7 seconds at periods of 8-, 16-, and 24-seconds, respectively. The increase in the spatial extent of the group velocity maps is apparent. With only one month of data, however, the imaged features in southern California appear to correlate well with those resulting from the twenty-two month data stack, particularly at the shorter periods. At short periods, therefore, structural information may be obtained from relatively short time series. The 75 km resolution contour provides an approximate boundary for the tomography. A frustrating result of continental imaging without ocean bottom seismometers is the poor resolution at the edges of the continents because of the absence

of paths crossing the coastline.

Features appearing in the 8-, 16-, and 24-second period group velocity maps correlate well with known geological structures. The 8-second period Rayleigh waves are most sensitive to the upper 10 km of the crust. At this period, the group velocity maps clearly show the plutonic and volcanic rocks of the Sierra Nevada Mountains and the Peninsular Range, and faster anomalies begin to appear for the Cascade Range. The high velocity regions for the Sierras and the Oregon Cascade Range are located slightly west of the mountain range axes. The thick sedimentary deposits of the Central Valley, Salton Trough, and Los Angeles and San Bernardino Basins are apparent from their low velocities.

The 16-second period Rayleigh waves are sensitive to structures in the upper and middle crust. The Sierras and Peninsular ranges remain prominent with high velocities. The Cascades show a clearer, uniform high velocity, extending from their southern extent into Washington where data resolution disintegrates. The Central Valley sediments are now clearly separated into the San Joaquin Basin in the south and the Sacramento Basin in the north. The high velocity anomaly running along the coast south of San Francisco defines the Salinian block and maps the trace of the San Andreas Fault.

At the 24-second period, Rayleigh waves are sensitive to the lower crust and have some sensitivity to crustal thickness. At these depths, the Sierras remain a high velocity feature. Large areas of Nevada are observed to be slow relative to the model average, perhap reflecting a warm lower crust or a thin crust. The northern extent of the Gulf of California is fast and suggests that the crust is significantly thinned where the North American continent meets the Gulf.

## Conclusions

This work applies the ambient noise surface wave tomography technique to emerging data from the EarthScope USArray Transportable Array in the western United

States. Using data collected between October 2004 and July 2006, we have generated cross-correlations between all receiver pairs, measuring group velocities between 5- and 50-second periods and carrying out tomographic inversions for group velocity maps at 8-, 16-, and 24-second period. The resulting group velocity maps reveal many velocity anomalies that are correlated with known geological features. The expansion of the TA during the twenty-two month study period resulted in a significant increase in the spatial extent of the group velocity maps. Using a resolution value of 75 km, the regions of high resolution at 8-, 16-, and 24-second periods increased by factors of five to seven between October 2004 and July 2006.

The application of ambient noise tomography to the USArray TA data presents a unique opportunity to study the crust and upper mantle of the United States. The technique produces high resolution images of the area covered by the footprint of the network. Measurements below 10 sec period are readily obtained. The limiting factors for improved resolution in the dispersion maps result from poor network coverage at the edges of the array and coastal margins. Further expansion of the TA will improve the resolution limitations at the northern and eastern edges of the group velocity maps presented here. Application of the method to phase velocities and Love waves and use of the resulting dispersion maps to infer the 3-D distribution of shear wave speeds in the crust and uppermost mantle are natural extensions of this study.

## Acknowledgments

The data used in this research were obtained from the IRIS Data Management Center and originate predominantly from the Transportable Array component of USArray. This research was supported by NSF grant EAR-0450082. MPM acknowledges a National Defense Science and Engineering Graduate Fellowship from the American Society for Engineering Education.

## References

Barmin, M.P., Ritzwoller, M.H., and Levshin, A.L (2001), A fast and reliable method for surface wave tomography, *Pure App. Geophys.*, *158*, 1351-1375.

Bensen, G.D., M.H. Ritzwoller, M.P. Barmin, A.L. Levshin, F.-C. Lin, M.P. Moschetti, N.M. Shapiro, and Y. Yang (2006), Processing seismic ambient noise data to obtain reliable broad-band surface wave dispersion measurements *Geophys. J. Int.*, submitted.

Cho, K.H., R.B. Hermann, C.J. Ammon, and K. Lee (2006), Imaging the crust of the Korean peninsula by surface-wave tomography, *Bull. Seism. Soc. Am.*, submitted.

Levshin, A.L., M.P. Barmin, M.H. Ritzwoller, and J. Trampert (2005), Minor-arc and major-arc global surface wave diffraction tomography, *Phys. Earth Planet. Ints.*, *149*, 205-223.

Ritzwoller, M.H. and A.L. Levshin, A.L. (1998), Surface wave tomography of Eurasia: group velocities, *J. Geophys. Res.*, *103*, 4839-4878.

Sabra, K.G., P. Gersotoft, P. Roux, W.A. Kuperman, and M.C. Fehler, (2005), Surface wave tomography from microseism in southern California, *Geophys. Res. Lett.*, *32* , L14311, doi:10.1029/2005GL023155.

Shapiro, N.M., M. Campillo, L. Stehly, and M.H. Ritzwoller (2005), High resolution surface wave tomography from ambient seismic noise, *Science*, *307*, 1615-16 18.

Shapiro, N.M., M.H. Ritzwoller, and G.D. Bensen (2006), Source location of the 26 sec microseism from cross correlations of ambient seismic noise, *Geophys. Res. Lett.*, in press.

Stehly, L., M. Campillo, and N.M. Shapiro (2006), A study of the seismic noise from its long range correlation properties, *J. Geophys. Res.*, in press.

Yang, Y., M.H. Ritzwoller, and A.L. Levshin (2006), Ambient noise Rayleigh wave tomography across Europe, *submitted Geophys. J. Int.*

Yang, Y. and M.H. Ritzwoller (2006), Source properties of ambient noise in Europe, in preparation.

Yao, H., R.D. van der Hilst, and M.V. de Hoop (2006), Surface-wave tomography in SE Tibet from ambient noise and two-station analysis: I. – Phase velocity maps, *Geophys. J. Int., 166*, 732-744.

Received _____

**Table 1.** Number of paths rejected prior to group velocity map inversion at 8-, 16-, 24-sec periods

| *Period* | 8 sec | 16 sec | 24 sec |
|---|---|---|---|
| Total waveforms | 30261 | 30261 | 30261 |
| SNR rejections | 14723 | 11045 | 12291 |
| Distance rejections | 446 | 1843 | 3683 |
| Dispersion measurement failure | 710 | 217 | 181 |
| Time residual rejection | 1026 | 714 | 516 |
| Remaining measurements | 13356 | 16442 | 13590 |

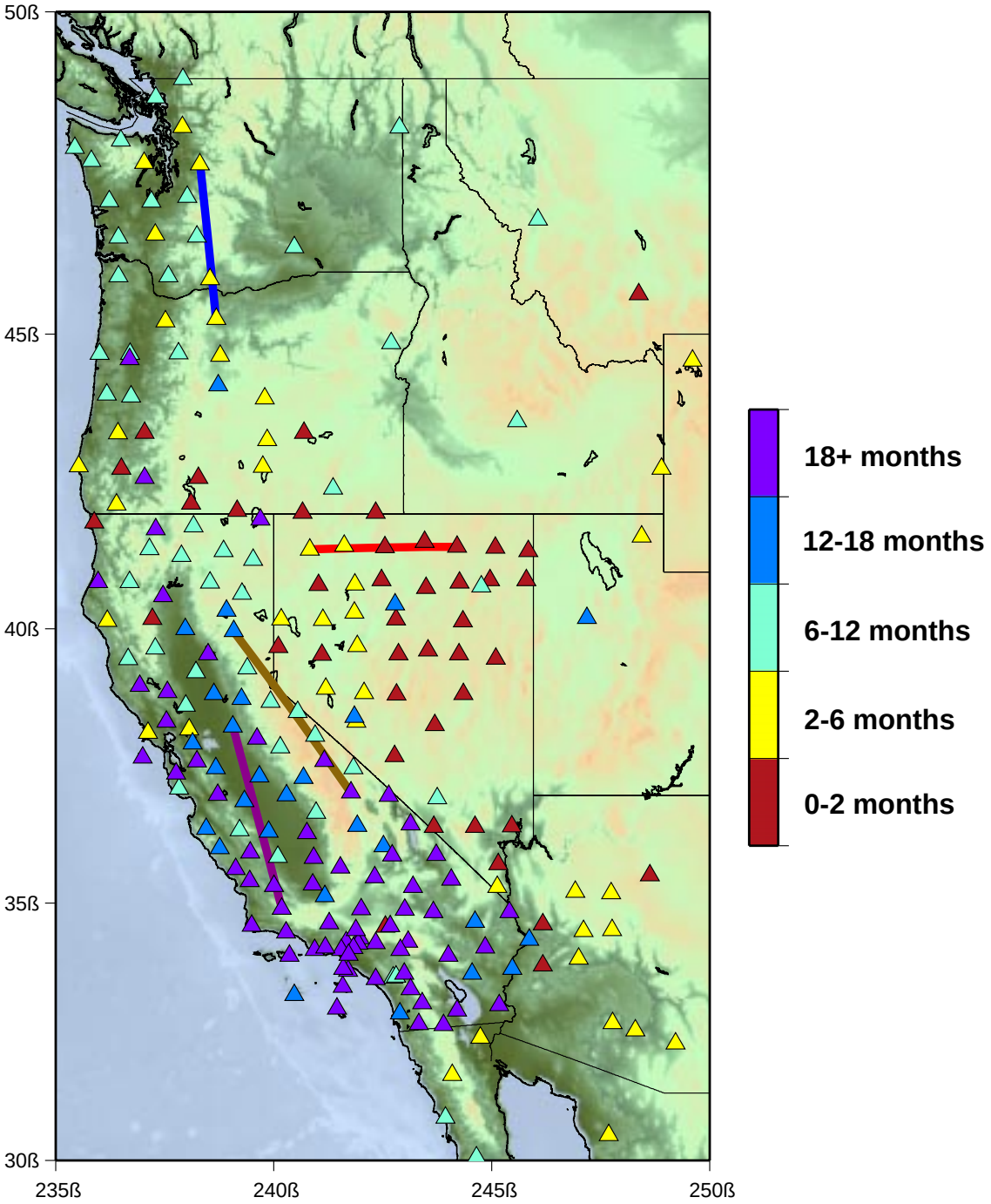


**Figure 1.** Study area and station distribution. Station symbol colors correspond to the duration for which data is available from the twenty-two month study period. Colored lines denotes wave paths for the cross-correlograms and dispersion curves shown in Fig. 2.

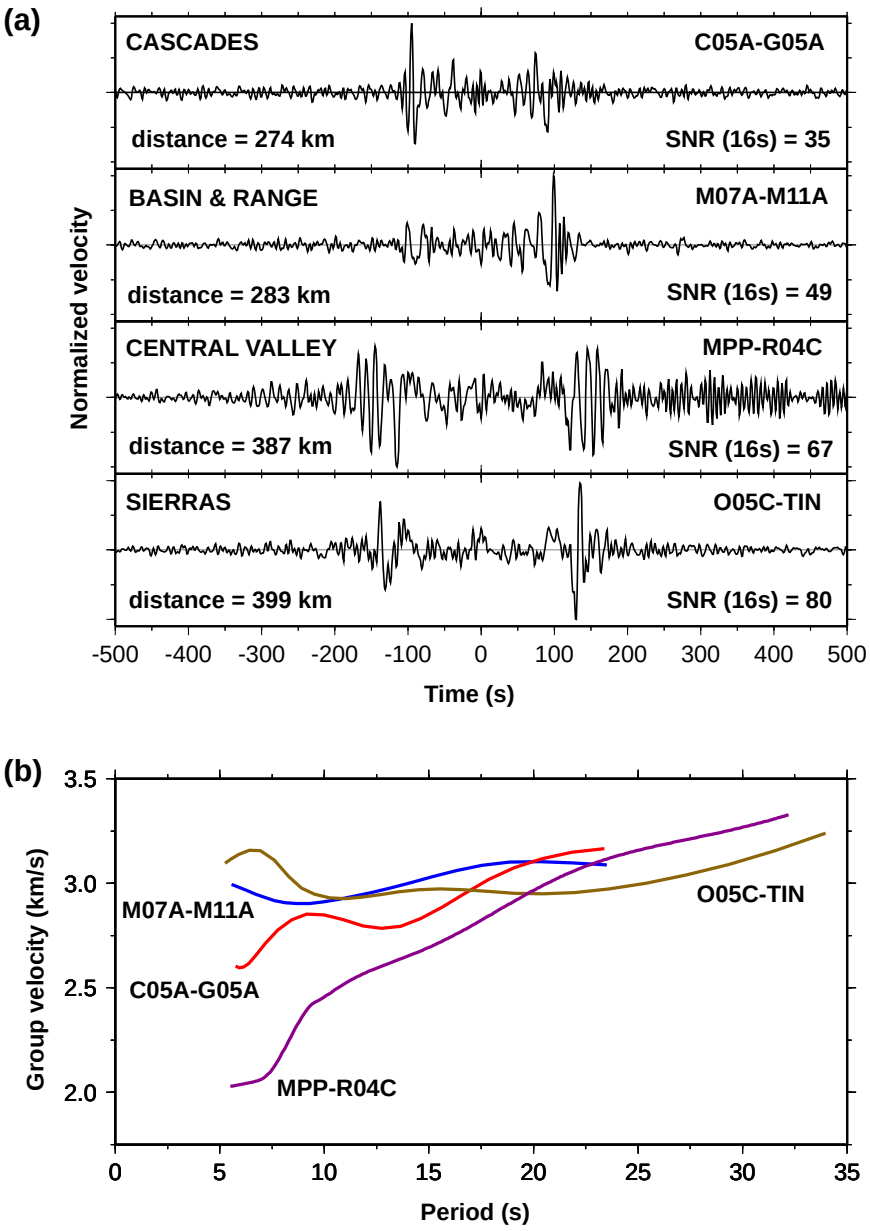


**Figure 2.** Cross-correlation waveforms and dispersion curves for the similarly colored wavepaths shown in Fig. 1. (a) The full, broadband cross-correlation waveforms are for the receiver pairs labeled. The waveforms result from time stacks of 3.4, 2.1, 17.5 and 13.6 months of data, respectively. (b) The dispersion curves are measured on the symmetric-component of the waveforms.

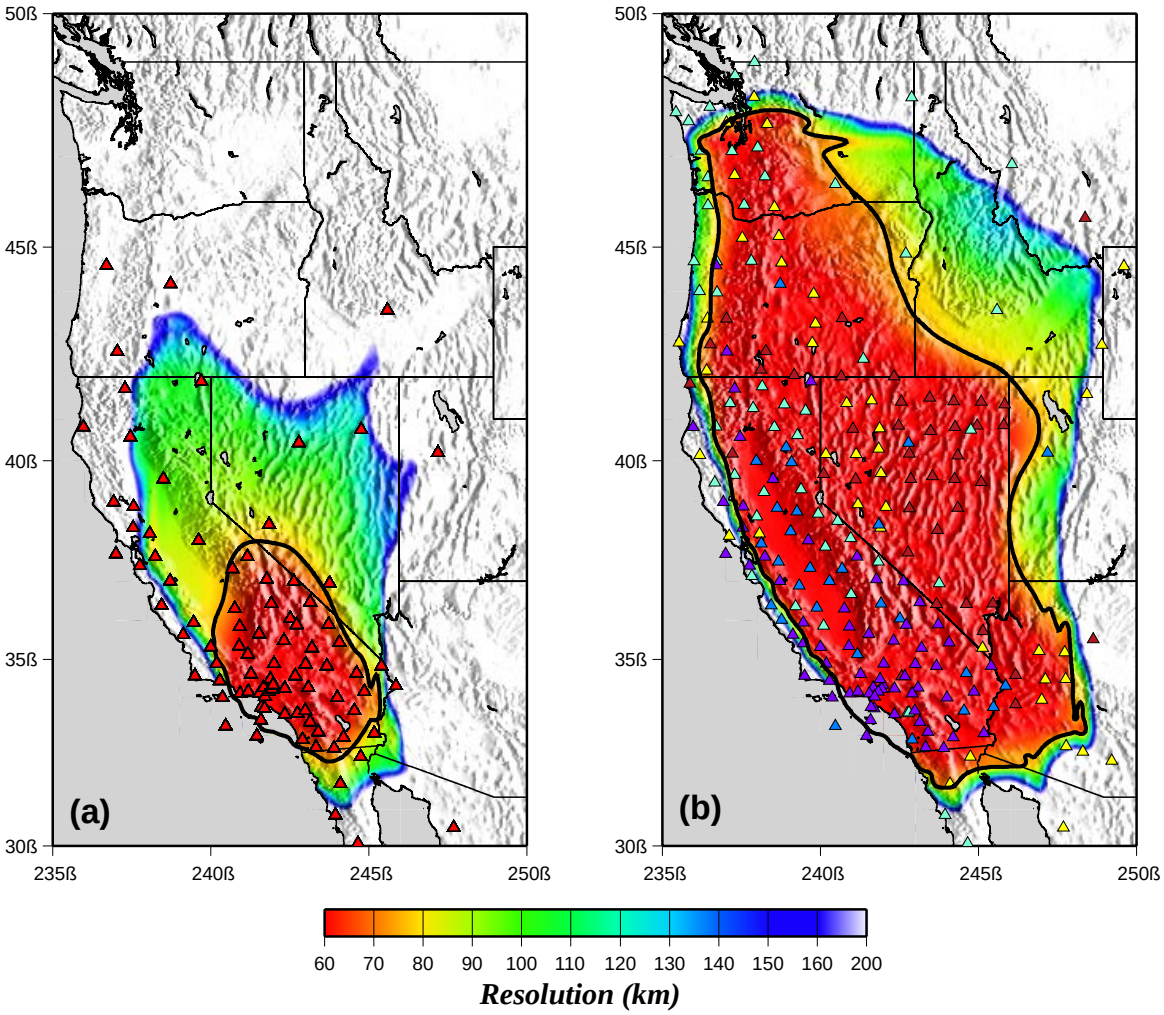


**Figure 3.** Comparison of the 8-second period resolution maps for one month of data from October 2004 and for 22 months of data from October 2004 through July 2006. (a) The resolution map at the 8-second period for October 2004. The 75 km resolution boundary is given by the black contour. (b) The resolution map at 8-second period for the October 2004 through July 2006 stack. Station symbols are color-coded to reflect the duration of operation, as in Fig. 1.

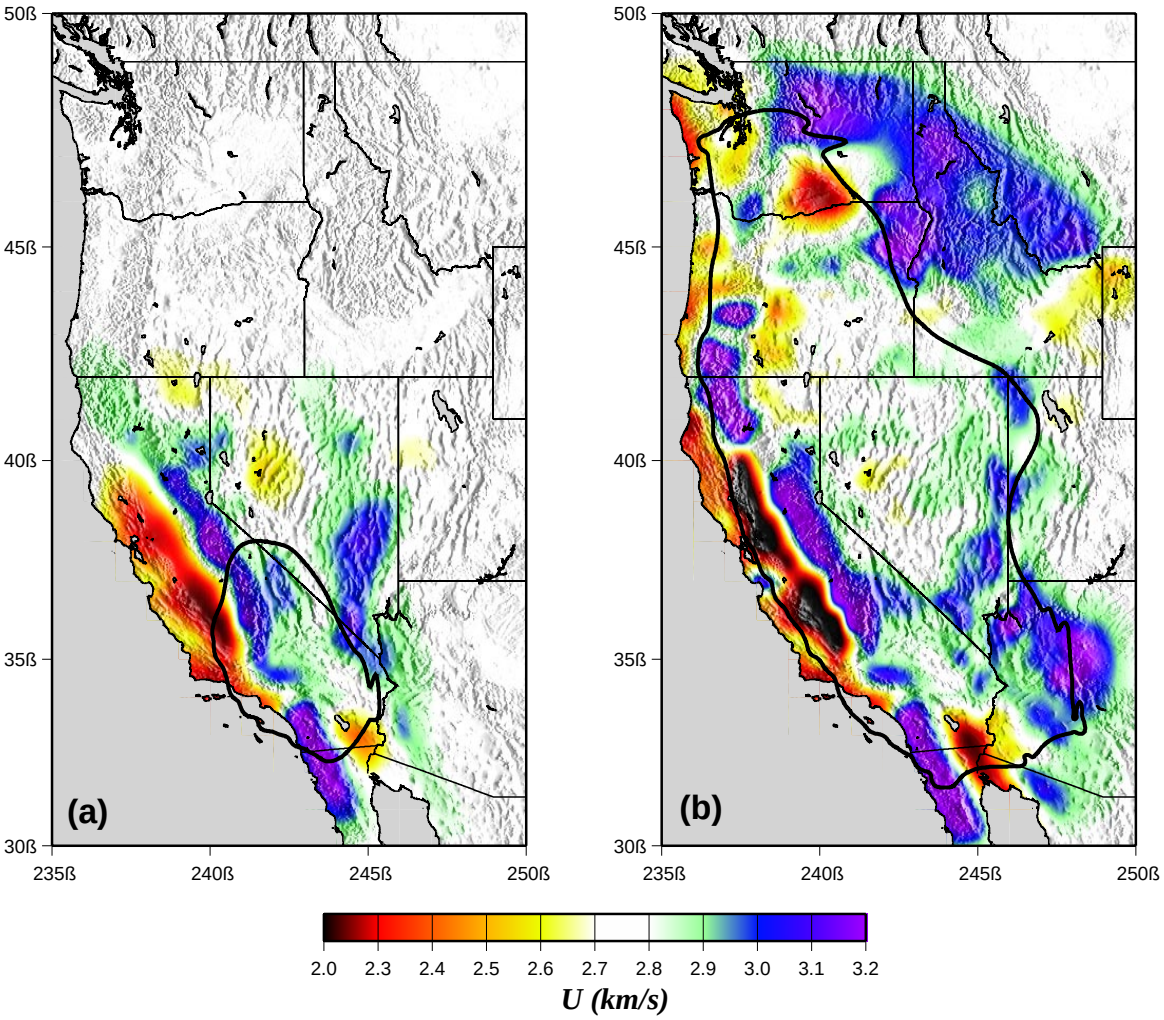


**Figure 4.** Comparison of the 8-second period group velocity maps from October 2004 and from October 2004 through July 2006. (a) The 8-second period group velocity map for October 2004. (b) The 8-second period group velocity map for the October 2004 through July 2006 stack. The 75 km resolution contour is drawn for reference in both panels.

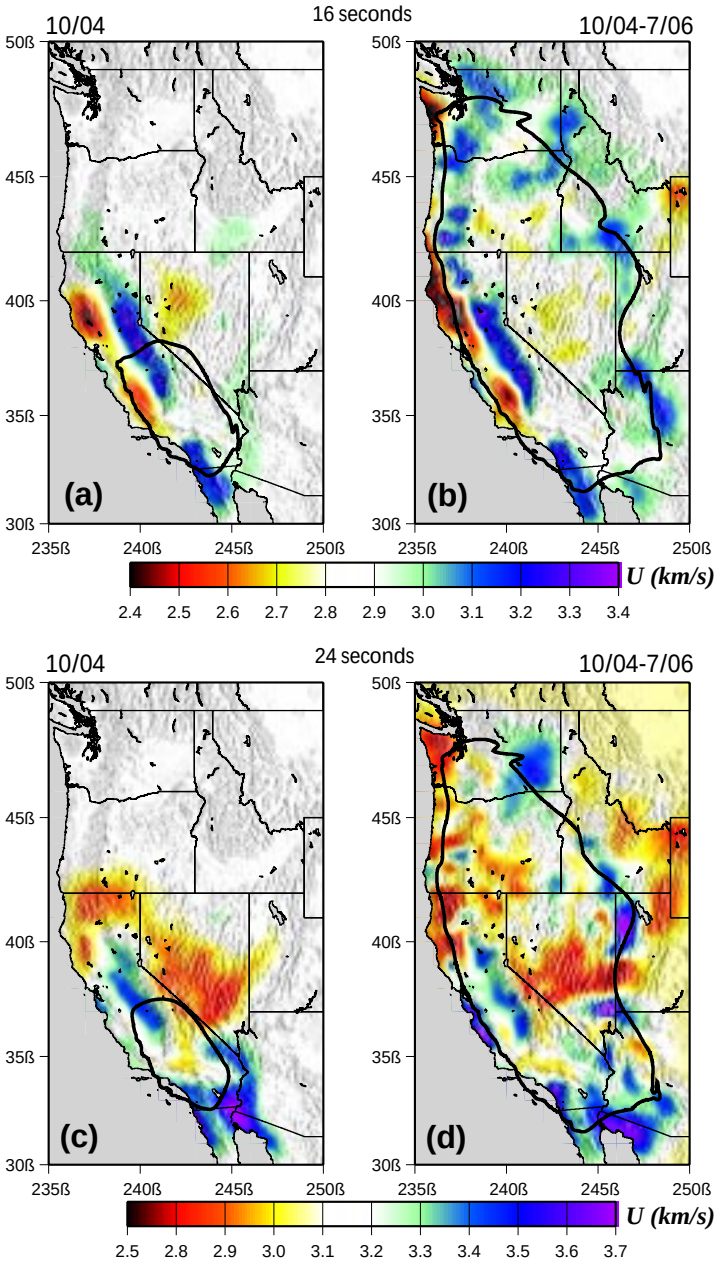


**Figure 5.** Comparison of the 16- and 24-second group velocity maps from October 2004 and from October 2004 through July 2006. (a) The 16-second period group velocity map for October 2004. (b) The 16-second period group velocity map for the October 2004 through July 2006 stack. (c) The 24-second period group velocity map for October 2004. (d) The 24-second period group velocity map for the October 2004 through July 2006 stack. The 75 km resolution contour is drawn for reference in all panels.